Australian Journal of Basic and Applied Sciences, 1(4): 415-430, 2007
ISSN 1991-8178

Utilization of a Large-Scale Testing Apparatus in Investigating and Formulating the Soil/Geogrid Interface Characteristics in Reinforced Soils

[1]Ahmed Hosny Abdel-Rahman, Mohamed Abdel-Moniem Ibrahim, [2]Alaa K. Ashmawy

[1]Dept., Eng. Research Division, National Research Center, Egypt.
[2]American University in Dubai, UAE

Abstract: A laboratory study was carried out using a large-scale universal testing apparatus to investigate the controlling factors affecting soil/geogrid interface shear strength, and conclude a representative mathematical formula for its prediction. The testing apparatus accommodates soil samples up to 1.0 m^3, and could perform direct shear tests on soils, pullout tests of geogrid sheets from soils, and uniaxial tension tests on the geogrid sheets without soils. Different types of geogrids, and punctured geomembranes sheets of different holes sizes were used in the testing program. Two different grain size distributions of cohesionless soils were also used in the testing program. The effect of the soil grain size distribution, its shear strength, dilatancy effect, geogrid surface configurations and material extensibility were investigated on the soil/geogrid interface shear strength. The results of the testing program as well as data reported in the literature were implemented to develop a formula to predict the soil/geogrid interface shear strength after incorporating the controlling factors.

Key Words: Reinforced Earth, Geogrid, Pullout, Interface, Shear Strength, Interlocking.

INTRODUCTION

Demands on geogrids as soil reinforcing materials have been rising since the last two decades. The mechanism of soil/geogrid interaction in reinforced earth has been one of the challenging geotechnical problems addressed in the literature; Sarsby (1985), Fannin *et al.,* (1993), and Ochiai *et al.,* (1996). The factors controlling the pullout resistance of a geogrid from soils are also widely addressed in the literature; Wilson-Fahmy *et al.,* (1994), Lopes *et al.,* (1996), Raju *et al.* (1997), and Abdel-Rahman (2000). Many mathematical formulas were proposed in the literature to predict the bond resistance between soils and geogrids; Hausmann (1977), Jewell *et al.* (1984), Milligan *et al.* (1987), and Abdel-Rahman (1997). Most of these formulas are not incorporating all the key parameters that are controlling the soil/geogrid interaction behavior such as grain size distribution, geometrical properties of the geogrid surface, and the extensibility of the geogrid material.

The effects of these factors were investigated through the results of a laboratory study conducted at the National Research Center of Egypt through a joint collaborative research effort with the University of South Florida, USA (Abdel-Rahman *et al.,* 2004). The research was funded from the US-Egypt Science and Technology Board (2001-2004). During the course of this research, a large-scale universal testing apparatus, that has the ability to run direct shear, pullout, and uni-axial tensile tests on soils and geosynthetics, was designed and manufactured at the National Research Center of Egypt. This apparatus was utilized to experimentally study the soil/geogrid interaction behavior.

Testing Program:

The following sections describe the testing apparatus, the basic properties of the materials used in the testing program, and the testing matrix.

Description of the Apparatus Used in the Testing Program:

Figure (1) presents an elevation view for the testing apparatus. The following sections briefly describe the components of the apparatus.

Corresponding Author: Ahmed Hosny Abdel-rahman, Dept., Eng. Research Division, National Research Center, Egypt.
E-mail: ahosny66@hotmail.com Fax: +202-2275-7417

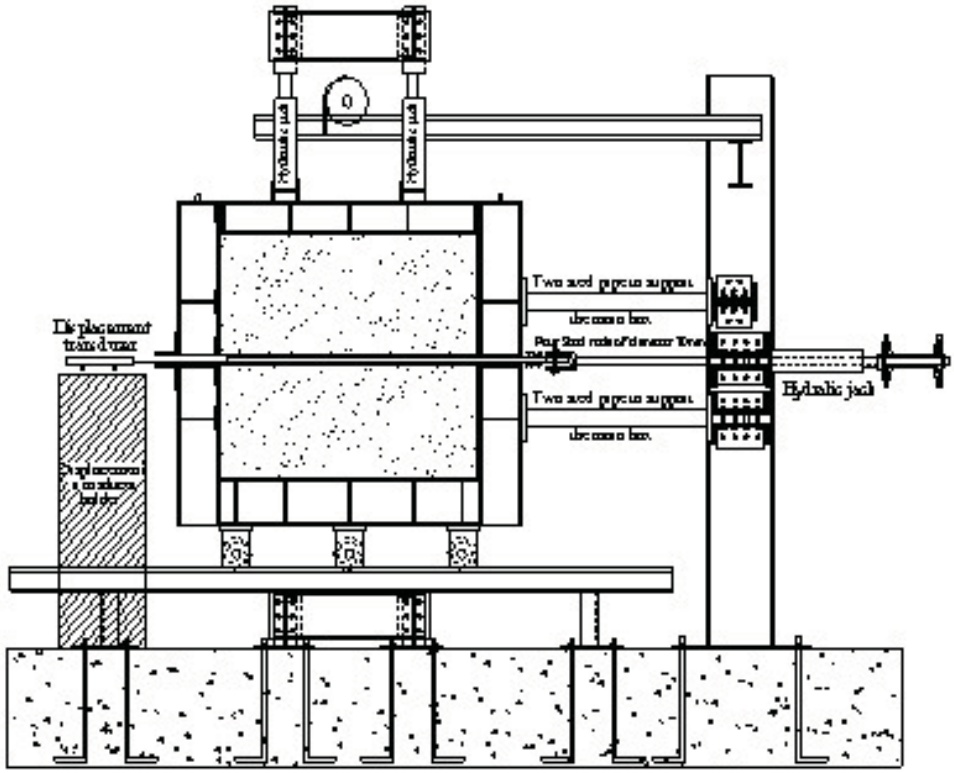

Fig. 1: An Elevation View for the Universal Testing Apparatus

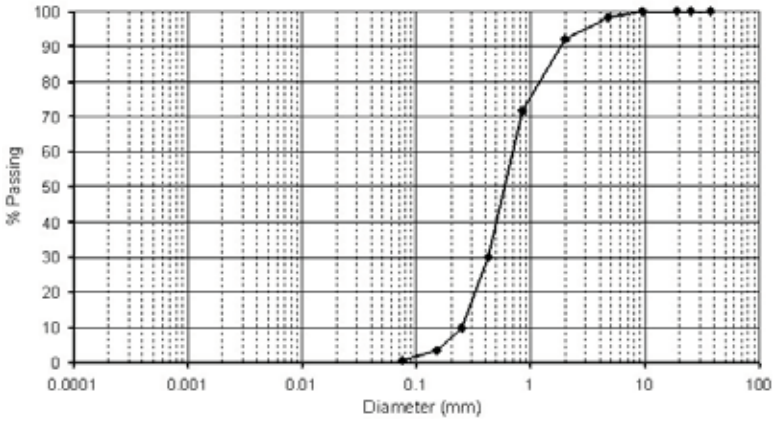

Fig. 2: The Grain Size Distribution of Soil (I)

The Main Box:

The Main Box, in which soils and geosynthetics samples are placed in, has inner dimensions of 1.20m x 0.70m x 1.16m for length, width, and height, respectively. It is divided into two main parts, upper and lower, spaced by a 4 cm gap. The lower box can be rolled to shear a soil sample while the top part is fixed in place by steel pipes as shown in Figure (1). Both parts of the box are fixed in place during pullout and uniaxial tensile tests.

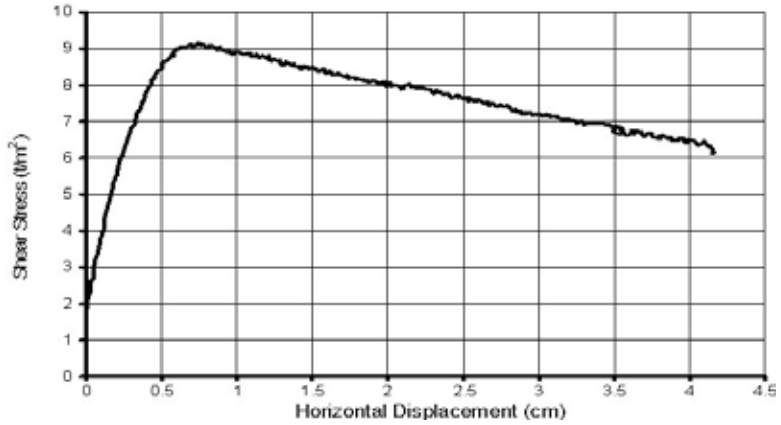

Fig. 3: Horizontal Displacement versus Shear Stress Relationship of Soil (I) under a Normal Stress of 14.8 t/m2.

Application of Vertical and Horizontal Forces:

A vertical reaction frame is designed to resist a total of 20 tons reaction forces from two vertical hydraulic jacks that simulate loads from in situ pressure. Another reaction frame is designed to resist a 25 ton horizontal force applied from a horizontal jack. That load could be used to pull a reinforcing sheet or to mobilize the lower box in a direct shear test.

The Instrumentation System:

Two pressure sensors, one is attached to the vertical loading system and the other is attached to the horizontal loading system, are used to automatically measure the vertical and the horizontal forces during their application. Two displacement transducers are used to measure the displacement at two different positions along the tested geogrid sheet. The displacement transducers are connected to the sheet using telltale wires. The telltale wires are encased in a very stiff steel pipes to avoid friction with the surrounding soils during testing. The pressure sensors and the displacement transducers are attached to an electronic data acquisition system.

Materials Used in the Tests:

Soils:

Two types of soils were used in the testing program. The first type, referred to herein as soil (I), was classified as medium to fine siliceous sand. That sand had an average grain size "D_{50}" of 0.60 mm, and a coefficient of curvature C_c of 1.03. A direct shear test, performed on that sand using the large-scale apparatus, showed that the angle of internal friction (Φ) is 32^o at 1.74 t/m^3 dry density and 94 % relative compaction. Figures (2) illustrate the grain size distribution of soil (I), while figure (3) presents its behavior during shearing in the large-scale apparatus.The second soil type, which will be referred to herein as soil (II), was classified as graded gravelly sand with some silt. This soil had an average grain size "D_{50}" of 0.55 mm, and a coefficient of curvature C_c of 0.85. A direct shear test, performed on the large-scale apparatus, showed that the angle of internal friction (Φ) is 37^o at 1.95 t/m^3 dry density and 95 % relative compaction. Figure (4) illustrate the grain size distribution of soil (II), while figure (5) presents its behavior during shearing in the large-scale apparatus.

Geogrids:

Available types of geogrids of different geometrical and mechanical properties were used in the laboratory-testing program; MEREX UL-90, MEREX UL-150 and TENAX TT. Figure (6) illustrates the notations used to identify the geometry of the different geogrids sheets. Table (1) presents the properties of these geogrids.

H.D.P.E Geomembranes:

Samples of geomembrane sheets of thickness 2mm and 3mm were punctured to different holes dimensions to

form geogrids of different holes dimensions and thicknesses. Table (2) shows the configurations of the different samples, and the opening ratios.

Pullout Testing Methodology:

The steps to perform a pullout test in the large-scale apparatus are briefly summarized as follow:

- The first two layers of soil are filled in the lower part of the box, each of thickness 25 cm, compacted to the required degree of compaction. Sand cone tests (ASTM 1556) are carried out to determine the soil density and relative compaction at the interface surface.
- Place the geogrid sample in its position in the apparatus. The recommended net dimensions of the tested part of the sample, excluding area to be clamped, are 0.90 m length x 0.60m width.

Table 1: Characteristics of the Tested Geogrid Sheets

Sample No	b (mm)	h (mm)	t (mm)	$^{*}\alpha_o$ (%)	Ultimate Tensile Strength	
					Machine Direction	Transverse Direction
MEREX UL-90 (Bi-axial)	19	31	1.25	74	9.0 t/m	2.0 t/m
MEREX UL-150 (Bi-axial)	15	31	1.75	52	13.0 t/m	2.6 t/m
TENAX TT (Uni-axial)	15	220	2.50	75	4.5 t/m	NA

$^{*}\alpha_o$ = Opening ratio of the geogrid defined as the area of the holes to the gross area of the sheet

Table 2: Holes Dimensions in Geomembrane Sheets of Thickness 2mm and 3mm

Sample No	b (mm)	h (mm)	t (mm)	Opening Ratio (%)
1(Unpunctured)	0	0	3	0
2	45	45	3	53
3	30	100	3	50
4	100	100	2	60
5	60	60	2	49
6	50	100	2	55
7	30	100	2	50
8	45	45	2	53

Table 3: Summary of the Tests Results Conducted on Punctured Geomembranes Sheets with Soil Type (I)

Test Number	b (mm)	h (mm)	t (mm)	Normal Stress (t/m^2)	Max. Shear Stress (t/m^2)
1	0	0	3	4.63	1.01
				11.26	1.57
				13.81	1.79
2	45	45	3	2.46	0.92
				4.62	1.05
3	30	100	3	2.11	1.27
4	100	100	2	0.80	0.43
5	60	60	2	0.80	0.65
6	50	100	2	0.80	0.69
7	30	100	2	0.80	0.74
8	45	45	2	0.80	0.6

- The telltales of the displacement transducers are secured at two positions on the tested sheet. One at its loaded edge and the other is located away from the loaded edge. The distance between the location of the front telltale and the rear one was different in each test according to the sheet configuration and holes dimensions. The pressure sensors and the displacement transducers are connected to the data acquisition system.
- Continue filling the remaining two soil layers above the geogrid sample, compacted to the required degree of compaction, and tested using the sand cone tests.
- The vertical loads are applied by two hydraulic jacks on top of a rigid plate placed on top of the soil in the upper part of the box.
- The pullout load is applied to the sample through a horizontal hydraulic jack while both parts of the box are fixed in place, during the horizontal load application, by strutting against a steel frame.

The Testing Matrix and Reduction of Results:

The testing program, shown in Figure (7), was designed to cover all the studied factors that affect the soil/geogrid interface shear strength including sheet configuration, extensibility, and soils types. In the figure, the machine direction of the sheet is referred to as "M.D", while the transverse direction of the sheet is referred to as "T.D". The interface shear strength per unit gross area of the sheet(τ_{ult} vas calculated in each test as follows:

$$\tau_{ult} = \frac{P}{2A} \quad \ldots\ldots\ldots\

Where:

ϵ	The average strain along the front part of the sheet,
$R_{(1)}$ and $R_{(2)}$	The readings of the front and the rear LVDT's, and
D	Distance between the front and rear LVDTs.

The coefficient of interaction (α) is defined as:

$$\alpha=(\tau_{ult}/\sigma_n).....(3)$$

Where:

τ_{ult} The interface shear strength, and

σ_n The applied normal stress at the interface level.

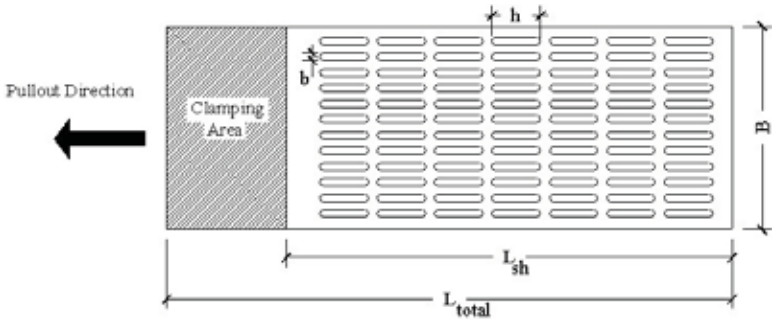

Fig. 6: Notations Used to Identify the Geometry of Different Geogrids

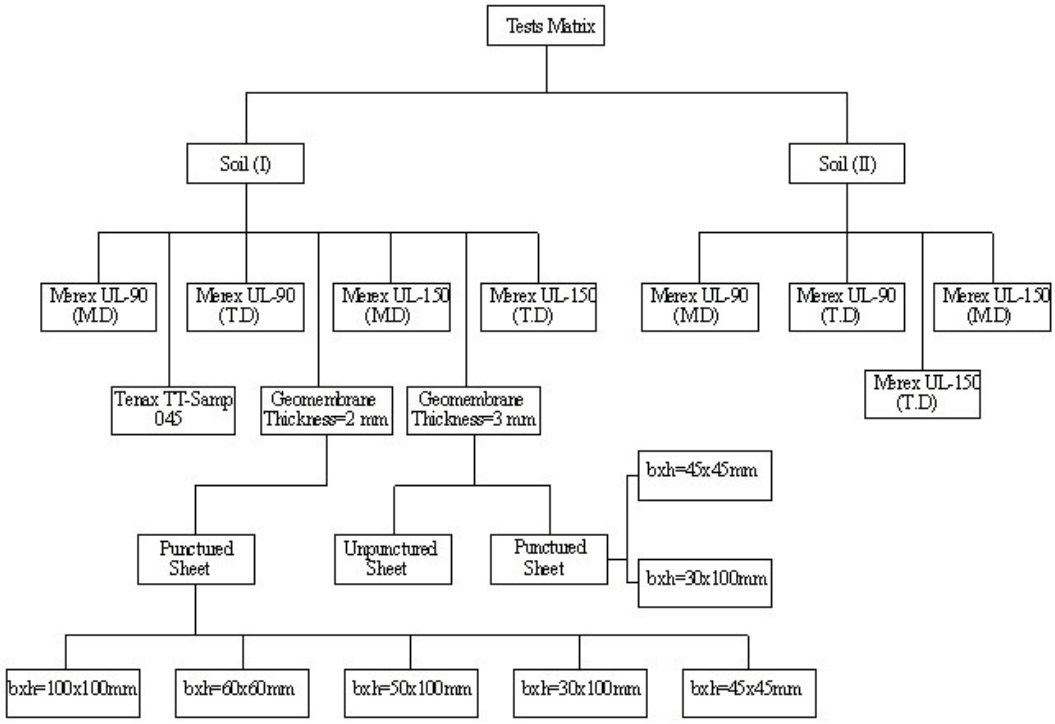

Fig. 7: Matrix of the Tests Conducted in the research Using Different Types of Soils and Geogrids

Pullout Tests Results:

Geogrid Merex UL-90 and UL-150:

The MEREX UL-90 and UL-150 geogrids were tested with soil (I) and (II) under different normal stresses that ranged between 0.8 ton/m^2 and 4.75 ton/m^2. The tests were repeated for cases where the sheets were in their machine direction and transverse directions. Figures 8 to 11 illustrate typical relationships depicted from these tests between the pullout force and the front displacement under different values of normal stresses.

Tenax TT Geogrid:

This geogrid type was tested with soil type (I) under normal stresses ranges between 1.85 ton/m^2 and 7.40 ton/m^2. The relationships between the pullout forces versus the front displacements, under each normal stress, are shown in figure (12).

H.D.P.E Geomembranes:

These tests were conducted to illustrate the effect of the bearing width (b) on the interaction of the soil with the reinforcement sheets. The tested geomembrane samples were of thickness 2mm, and 3 mm. All tests were conducted with soil type (I). Table (3) summarizes the tests results.

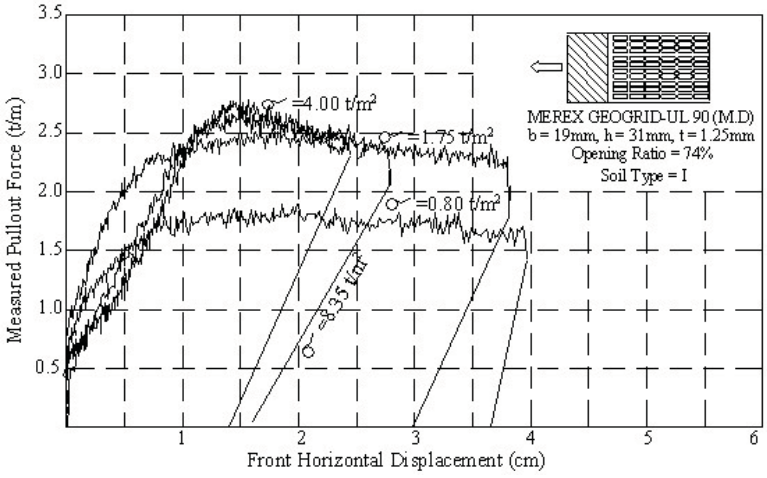

Fig. 8: Relationship between Pullout Force and Front Horizontal Displacement (UL-90 - M.D. - Soil I)

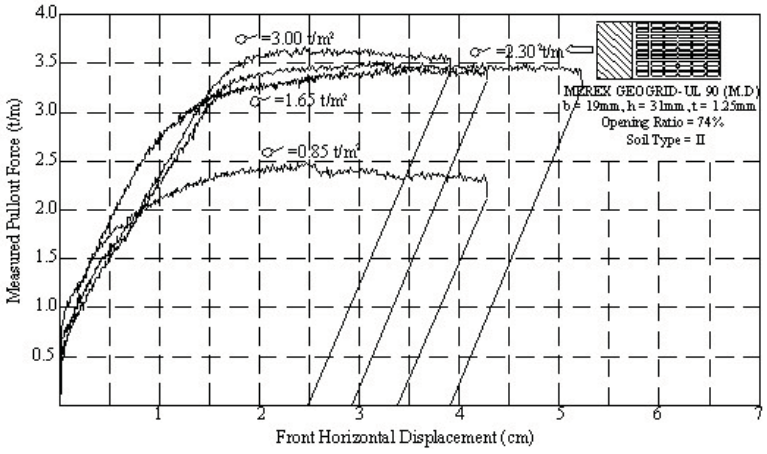

Fig. 9: Relationship between Pullout Force and Front Horizontal Displacement (UL-90 -M.D. - Soil II)

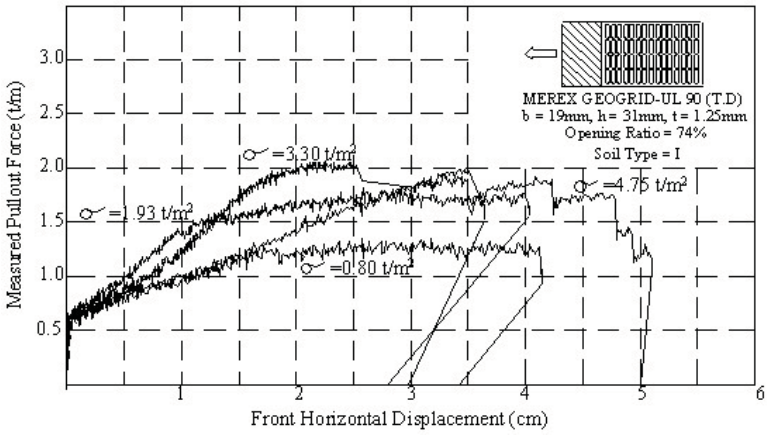

Fig. 10: Relationship between Pullout Force and Front Horizontal Displacement (UL-90 - T.D. - Soil I)

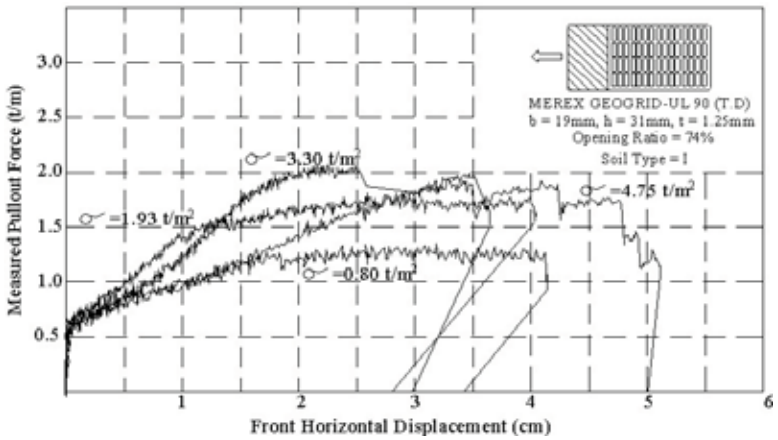

Fig. 11: Relationship between Pullout Force and Front Horizontal Displacement (UL-90 - T.D. - Soil II)

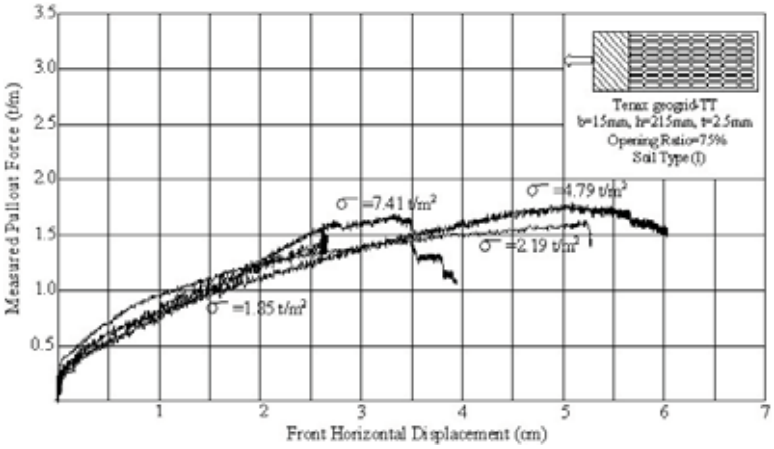

Fig. 12: Relationship between Pullout Force and Front Horizontal Displacement (TENAX -TT - Soil I)

Factors Affecting Soils/geogrids Interface Shear Strength:

The effect of the parameters pertaining to soil and geogrid properties on the mechanical behavior of soils/geogrids interaction will be analyzed using the tests results. The dominating parameters were classified as follows:

- Parameters pertaining to soil physical and mechanical properties: shear strength characteristics, grain size distribution, and dilatancy effect.
- Parameters pertaining to geogrid geometrical and mechanical properties: internal dimensions of grid apertures, thickness of geogrid transverse ribs, flexure rigidity of the geogrid transverse ribs, and the extensibility of the geogrid material.

Investigating the Parameters Pertaining to Soil Physical and Mechanical Properties:

Grain Size Distribution: To investigate the effect of grain size distribution, the results of the tests conducted on the geomembrane sheets were used to evaluate the effect of the ratio (b/D_{50}) on the efficiency factor (E); where the efficiency factor is defined as:

$$E = \frac{\tan\delta}{\tan\Phi} \times 100 \quad \ldots\ldots\ldots\

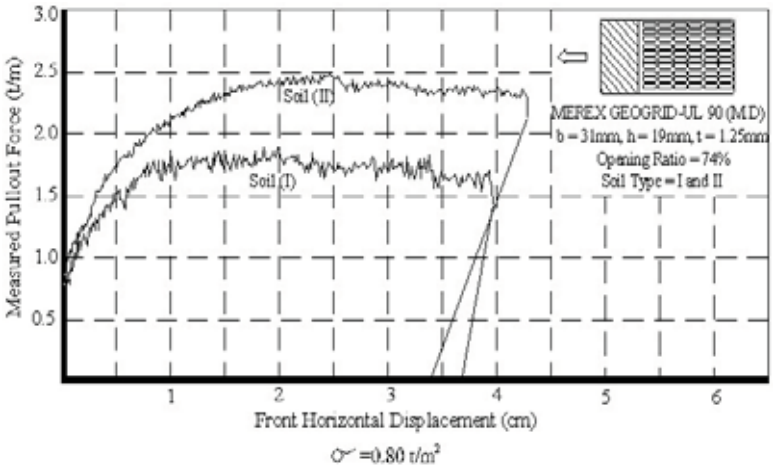

Fig. 14: Relationship between Pullout Force versus Front Displacement for Geogrid MEREX UL-90 When Tested with Soils (I and II) Under Similar Testing Conditions

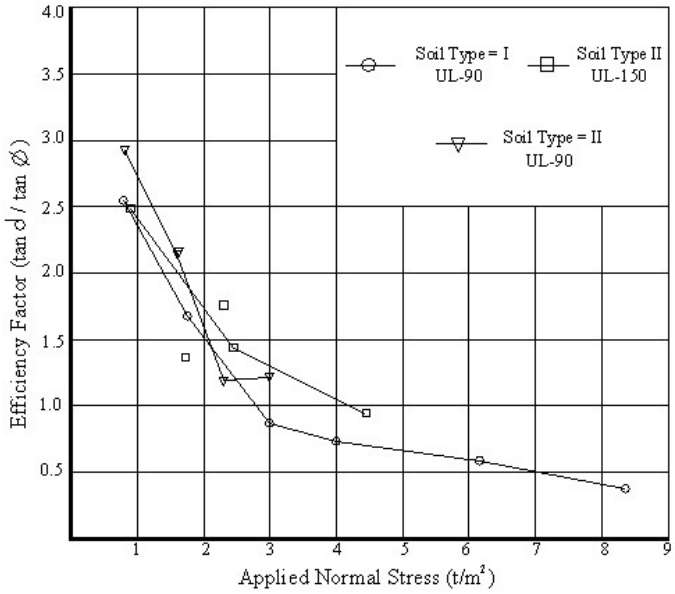

Fig. 15: Effect of the Normal Stress on the Efficiency Factor for Various types of Geogrids and Soils

sheets. Also, the relationship between (b/D_{50}) versus the efficiency factor (E) is presented in figure (13), where "b" is denoted as "b_g". From figure (13), it can be seen that the efficiency factor increases with increasing the value of (b/D_{50}) till a maximum value of about 50, then the efficiency factor decreases with increasing (b/D_{50}) afterwards. That means, for soil (I) of D_{50} = 0.6 mm, the optimum width of geogrid t o provide interlocking with soils is 30 mm.

Shear Strength Characteristics of the Tested Soils:

Geogrid MEREX UL-90 was tested with soils (I) & (II) under identical conditions of normal stresses, and loading rate. Figure (14) indicates an increase in the pullout resistance for case of soil (II) than soil (I) due to its higher shear strength parameter (Φ).

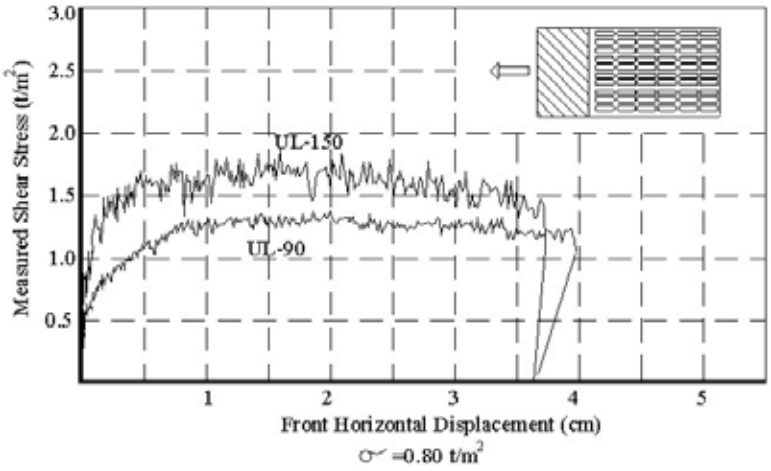

Fig. 16: Pullout Responses of Two Geogrids of Different Uniaxial Tensile Stress-Strain Characteristics under Similar Testing Conditions

Dilatancy and Relative Density of Soil: The dilatancy effect depends on the initial value of normal stress at the soils/geogrids interface (Farrag *et al.,* 1993). Soils tend to dilate at low normal stresses, while at a very high

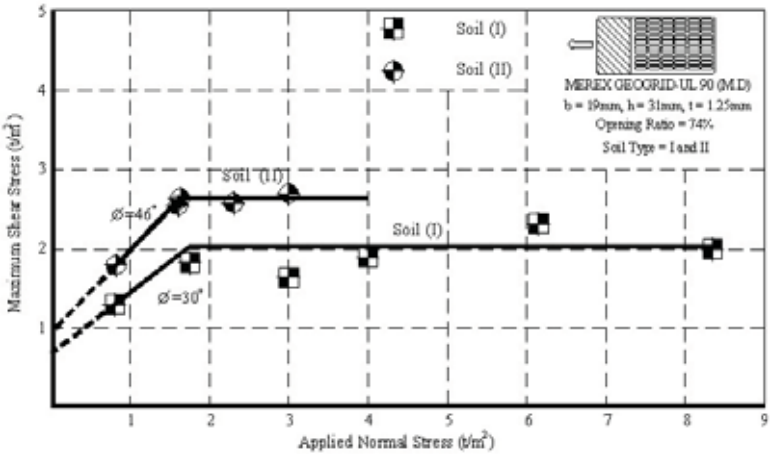

Fig. 17: Shear Strength versus Normal Stress Relationship for Geogrid MEREX UL-90 When Tested with Soils (I and II) Under Similar Testing Condition

normal stresses, the dilatancy effects are suppressed. This dilatancy is restrained by the top rigid plate, and so results in a normal stress increase at the soil/geogrid interface surface, thereby, increasing the pullout resistance (Juran *et al.,* 1988).

The tests results of geogrids MEREX UL-90 and MEREX UL-150 with the two types of soils are shown in figures (15). It can be seen that the value of the efficiency factor is greater than 1.0 for low normal stresses, then decreases with increasing the applied normal stress. It is worth noting that the cases where the efficiency factors are lower than 0.7 were experiencing early failures in the materials of the geogrids sheets.

Parameters Pertaining to Geogrid Properties:

Geogrid Geometrical Configuration:

The dimensions and aspect ratios of the geogrid holes affect the interlocking with soils (Abdel-Rahman, 1997).

The effect of the geogrids holes dimensions should be investigated in conjunction with the grain size distribution of the surrounding soils. Accordingly, the same conclusion drawn earlier regarding the effect of (b/D_{50}) will apply. As a result, the ratio of geogrid hole width to soil grain size should be considered in the interface shear strength criterion.

The Extensibility of the Geogrid:

The variations in the geogrid response during pullout tests are controlled by their uni-axial tensile stress-strain performance in the unconfined conditions. The extensibility of the longitudinal members and the flexure rigidity of the transverse members influence the soils/geogrids interaction greatly (Wilson Fahmy *et al.,* 1994). Figure (16) presents tests results of two different geogrids performed under similar testing conditions including normal stress, and soil types. The following can be concluded from this figure:

- The tangent moduli for the case of the stiffer geogrid (UL-150) are higher than those for the relatively softer geogrid (UL-90).
- A higher pullout force is obtained in the case of stiffer geogrid (UL-150).
- Less horizontal displacement, for the same load, was acquired in the case of stiffer geogrid (UL-150) due to the high flexure rigidity of its transverse ribs.

Soil-geogrid Interface Shear Strength:

As shown in figure (17), the relationship between the applied normal stress and the interface shear strength reaches to a limit where it gets constant afterwards depending on the sheet mechanical properties. This behavior

Table 5: Photos of some failure patterns in the tested geogrid sheets Loading Direction

Loading Direction	Photo	Comments
Loading in the Machine Direction		Rupture due to tensile failure in the longitudinal ribs
		Failure in the Junctions (shear failure) between the longitudinal and transverse ribs.
Loading in the transverse Direction	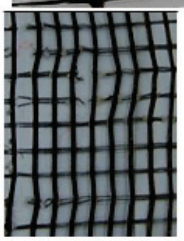 (a) 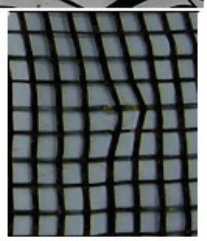 (b)	(a) Rupture in the rips due to tensile failure (b) Flexure failure in the transverse ribs due to interlocking with soils

was typical when investigated for the tests results of all other types of geogrids and soils. It could be attributed to inadequate strength of the geogrid materials to transfer the pullout loads to soils. Possible limitations in the geogrid strength could be as follows:

- Tensile failure in the longitudinal ribs.
- Flexure failure or shearing failure along the transverse ribs.
- Failure due to inadequate junction strength between the longitudinal and the transverse ribs.

Table (5) shows photos for typical failure mechanisms experienced during the course of this research.

Prediction of the Interface Shear Strength (T_{ult}):

The author (Abdel-Rahman, 1997) introduced a general equation to model different interactions between soils and geosynthetics considering the geometrical nature of the geogrid holes as follows:

$$\tau_f = (1-\alpha_o)(C+\sigma_n \tan\Phi) + 0.5\alpha_o \frac{t}{h}(CN_c + \sigma_n N_q) \quad \ldots\ldots\ldots\ldots\ldots\ldots\ldots\ldots (5)$$

Where:

τ_f	interface shear strength uniformly distributed per unit planner area of the sheet,
α_o	geogrid opening ratio,
C and Φ	interface shear strength parameters,
σ_n	normal stress on the interface surface,
t	thickness of geogrid bearing member,
h	hole length that is normal to the bearing width (b), and
Nc and Nq	bearing capacity factors, where N_c is considered zero for cohesionless soils.

Abdel-Rahman (1997) used the proposed equation by Chai (1992) to express the bearing capacity factor N based on Vesic's (1963) postulates for a punching failure of a deeply embedded foundation; such that:

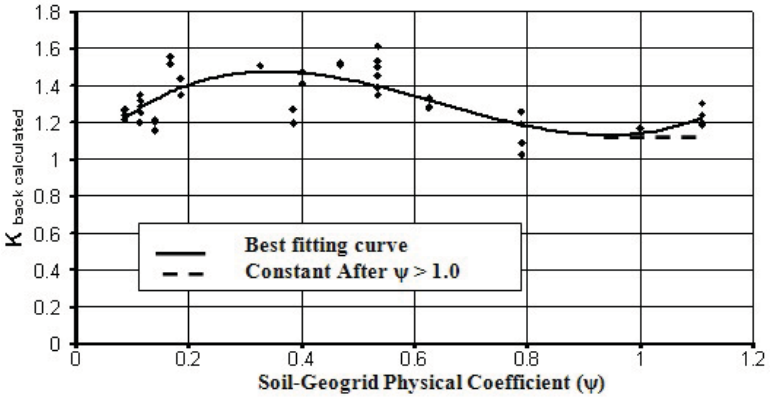

Fig. 18: The Relationship between the Back Calculated Interaction Factor (K) and the soil-geogrid physical coefficient (Ψ)

$$N_q = \left(\frac{1}{\cos\Phi}\right) e^{\pi \tan\Phi} \tan\left(45 + \frac{\Phi}{2}\right) \quad \ldots\ldots\ldots\ldots\ldots\ldots\ldots\ldots (6)$$

A parametric study was performed on equation (5) using 27 case history, well documented in the literature and its predictability was proven to be in the acceptable ranges (Hamed, 2004). However, the bearing factor (N_q),

defined in Eqn (6), depends only on the soil friction angle and neglects other factors related to soil grain size, holes dimensions of geogrids, and thickness of the bearing members.

To overcome the shortcomings of the recommended equation (Abdel-Rahman, 1997), the tests results performed in this research, and other data collected from the literature, were used to introduce other parameters in its terms. Table (6) summarizes the cases used in the analyses. The mathematical derivation to reach a more representative definition is explained in details in the following sections.

Enhancing the Bearing Capacity Factor (N_q) in the Recommended Equation: The bearing capacity factor (N_q) could be defined as the ratio between the bearing stress acting against the transverse ribs to the normal stress on the interface. Accordingly, the parameters affecting the bearing resistance should be considered in the mathematical representation of the soil/geogrid interface. These parameters are; the bearing element length (b), the thickness (t) of the transverse (bearing) ribs, the soil grain size (D_{10} and D_{60}), and the soil friction angle (Φ).

These factors were considered to develop a different interface angle (Φ_b), related to the soil friction angle (Φ) by a coefficient (k); such that:

$$\Phi_b = (k)*(\Phi) \quad \ldots\ldots(7)$$

Where:

Φ The angle of internal friction of the soil, and

k The soil/geogrid interaction factor.

The controlling parameters are assembled into one factor, defined as the soil-geogrid physical coefficient (ψ). The soil-geogrid physical coefficient is computed according to equation (8) as follows:

$$\psi = \left(\frac{t \times D_{60}}{b \times D_{10}} \right) \quad \ldots\ldots(8)$$

Both parameters "K" and "ψ" were computed from the measurements of each case history, presented in table (6), according to equations 7 and 8, respectively. Φ_b is back-calculated using equations 5 and 6 knowing all the required parameters. The relationship between the back calculated interaction factor (k) and (ψ) is shown in figure (18).

Table 6: Tests Results Considered in the Deriving the Equation of Interaction Factor (k)

No	Reference	*Geogrid Types	b (mm)	h (mm)	**α_o (%)	t (mm)	σ_n (t/m^2)	Φ(°)	τmeasured(t/m^2)
1	Wilson Fahmy et al (1994)	N/A	15	137	57	5.8	6.9	35	4.35
2	Raju et al (1997)	N/A	17	145	60	4.3	1.0	31	1.08
3	Raju et al (1997)	N/A	17	145	60	4.3	1.70	31	1.7
4	Raju et al (1997)	N/A	22	23	60	1.6	0.40	31	0.4
5	Raju et al (1997)	N/A	22	23	60	1.6	1.0	31	1.08
6	Raju et al (1997)	N/A	22	23	60	1.6	1.70	31	1.78
7	Raju et al (1997)	N/A	20	58	46	2.1	0.40	31	0.50
8	Raju et al (1997)	N/A	20	58	46	2.1	1.00	31	1.30
9	Lopez et al (1996a)	G-1	16	140	59	2.6	4.67	35.7	2.45
10	Lopez et al (1996a)	G-1	16	140	59	2.6	4.67	35.2	1.69
11	Lopez et al (1996b)	G-1	16	140	59	2.6	2.60	40	1.14
12	Lopez et al (1996b)	G-1	16	140	59	2.6	4.67	41	1.68
13	Abdel-Rahman *et al.* 2004	G-2	19	31	74	1.25	0.80	32	1.30
14	Abdel-Rahman *et al.* 2004	G-2	19	31	74	1.25	1.75	32	1.830
15	Abdel-Rahman *et al.* 2004	G-2	19	31	74	1.25	1.63	37	2.64
16	Abdel-Rahman *et al.* 2004	G-2	19	31	74	1.25	0.80	37	1.80
17	Abdel-Rahman *et al.* 2004	G-2	19	31	74	1.25	1.60	37	2.55
18	Abdel-Rahman *et al.* 2004	G-3	31	19	74	1.25	0.80	32	1.35
19	Abdel-Rahman *et al.* 2004	G-3	31	19	74	1.25	1.93	32	1.81
20	Abdel-Rahman *et al.* 2004	G-3	31	19	74	1.25	0.85	37	2.08
21	Abdel-Rahman *et al.* 2004	G-3	31	19	74	1.25	1.70	37	2.80
22	Abdel-Rahman *et al.* 2004	G-4	15	31	52	1.75	0.80	32	1.86
23	Abdel-Rahman *et al.* 2004	G-4	15	31	52	1.75	0.90	37	1.66

Table 6: Continued

24	Abdel-Rahman *et al.* 2004	G-4	15	31	52	1.75	2.30	37	3.00
25	Abdel-Rahman *et al.* 2004	G-4	15	31	52	1.75	1.75	37	1.77
26	Abdel-Rahman *et al.* 2004	G-4	15	31	52	1.75	2.45	37	2.61
27	Abdel-Rahman *et al.* 2004	G-5	15	215	75	2.50	2.19	32	1.62
28	Abdel-Rahman *et al.* 2004	G-5	15	215	75	2.50	1.85	32	1.41
29	Senoon et al (2003)	G-6	15	215	75	2.50	0.325	35	0.318
30	Senoon et al (2003)	G-6	15	215	75	2.50	0.65	35	0.446
31	Senoon et al (2003)	G-6	15	215	75	2.50	0.975	35	0.531
32	Senoon et al (2003)	G-6	15	215	75	2.50	0.325	31	0.271
33	Senoon et al (2003)	G-6	15	215	75	2.50	0.65	31	0.375
34	Senoon et al (2003)	G-6	15	215	75	2.50	0.975	31	0.474
35	Tenax report GRID-TE-5	G-7	28	40	84	1.3	1.0	38	1.30
36	Tenax report GRID-TE-5	G-7	28	40	84	1.3	2.0	38	2.50
37	Tenax report GRID-TE-5	G-7	28	40	84	1.3	3.0	38	2.83
38	Tenax report GRID-TE-5	G-8	28	40	84	0.8	1.0	38	1.14
39	Tenax report GRID-TE-5	G-8	28	40	84	0.8	2.0	38	2.35
40	Tenax report GRID-TE-5	G-8	28	40	84	0.8	3.0	38	2.92
41	Tenax report GRID-TE-5	G-8	28	40	84	0.8	4.0	38	3.33

$^{**}\alpha_o$: Opening Ratio

*Geogrid Types Implemented in the Analysis

Symbol	Name	Symbol	Name
G-1	Tensar SR55	G-5	Tenax 45 (Pulled in Machine Direction)
G-2	UL-90 (Pulled in Machine Direction)	G-6	Tenax 60 (Pulled in Machine Direction)
G-3	UL-90 (Pulled in Transverse Direction)	G-7	Tenax SS2
G-4	UL-150 (Pulled in Machine Direction)	G-8	Tenax SS1

Figure (18) shows that the interaction factor (k) ranges between 1.00 and 1.60. This relationship was fitted in a polynomial equation of the third degree, as shown in the figure with a maximum of 1.50 and a minimum of 1.10. This third degree polynomial equation can be rewritten in the following form;

$$K = 3.25\ (\psi^3) - 6.3\ (\psi^2) + 3.2\ (\psi) + 1.0 \quad \ldots\ldots (9)$$

A recommended limitation on the value of (k) is to be a constant of 1.10 after a value of (ψ) greater than or equal to 1.0. On the other hand, it is recommended that the maximum value of (Φ_b) not to exceed 45^o to avoid numerical incompatibility with the nature of the problem.

Accordingly, the interface shear strength criterion can be rewritten as follow:

$$\tau_f = (1-\alpha_o)(C + \sigma_n \tan\Phi) + 0.5\alpha_o \frac{t}{h}(\sigma_n N_q) \leq \tau_{max} \quad \ldots\ldots (10)$$

N_q is to be calculated according to equation (6) considering $\Phi = \Phi_b$, where:

- $\Phi_b = (k)*(\Phi) \leq 45^o$
- $K = 3.25\ (\psi^3) - 6.3\ (\psi^2) + 3.2\ (\psi) + 1.0$
- $\psi = \left(\frac{t \times D_{50}}{b \times D_{10}}\right)$

τ_{limit} is the least of:

- τ_f as computed from equation (10).
- The tensile strength of the sheet material.
- The junction strength.
- The flexural strength of the transverse ribs.
- The shear strength of the transverse ribs.

Conclusions:

- In any reinforced earth structure, it is highly recommended to perform a large-scale pullout test using the same reinforcing sheet and soil that will be used on-site to study their interaction mechanism.
- The increase in the ratio of (b/D_{50}) results in an increase in the efficiency factor (E) till an optimum aperture ratio, then a decrease in (E) takes place. The optimum (b/D_{50}) was found in this research, for medium to fine siliceous sand, to be 50.
- The pullout resistance and the initial tangent modulus are higher for the stiffer geogrid than the relatively softer geogrid.
- The coefficient of interaction decreases with increasing the value of the applied normal stress due to suppressing the dilatancy effect.
- The bearing capacity factor (N_q) is not only controlled by the soil friction angle (Φ), but is also affected by the transverse ribs length, its thickness, and the soil particle size.
- The increase in the interface normal stress results in an increase in the interface shear strength till a certain value, (τ_{limit}), at which the interface shear strength remains constant. The value of the τ_{limit} depends mainly on the mechanical properties of the tested sheet such as; the strength of the longitudinal ribs, the junction strength and the transverse ribs rigidity.

REFERENCES

Abdel-Rahman, A., 1997. “Modeling of Soil/Geosynthetic Interaction in Reinforced Earthworks”, Ph.D. thesis, Dept. of Civil and Environmental Engineering, Tulane University.

Abdel-Rahman, A., 2000. “Factors Dominating Soil/Geogrid Interface Shear Strength”, Al-Azhar Engineering Sixth International Conference.

Abdel-Rahman, A.H. and A. Ashmawy, 2004. "Development of a Multi-Function Geosynthetic Testing Apparatus”. A Final Research Report submitted to the US-Egypt Science and Technology Board.

Chai, J.C., 1992. "Interaction between Grid Reinforcement and Cohesive-Frictional Soil and Performance of Reinforced Wall/Embankment on Soft Ground," Ph.D. Dissertation, Asian Inst. of Tech., Bangkok, Thailand.

Fannin, R.J. and D.M. Raju, 1993. “Large-Scale Pullout Test Results on Geosynthetics”, Vancouver, Canada-Geosynthetics.

Farrag, K., Y.B. Acar and I. Juran, 1993. “Pullout Resistance of Georgrid Reinforcements”, Geotextiles and Geomembranes, pp: 133-159.

Hamed, M.O., 2004. “Numerical Modeling of Reinforced Earth Structures”, M.Sc, Dept. of Civil Engineering, Cairo University.

Hausmann, M.R. and J.M. Vageneron, 1977. “Analysis of Soil-Fabric Interaction”, C.R. Coll. Int. Sols Textile, Paris.

Jewell, R.A., G.W.E. Milligan, R.W. Sarsby and D. Dubois, 1984. “Interaction between Soil and Geogrids”, In Proceedings of Symposium on Polymer Grid Reinforcement, Thomas Telford Limited, London, pp: 18-30.

Juran, I., G. Knochenmus, Y.B. Acar and A. Arman, 1988. “Pullout Response of Geotextiles and Geogrids”, Special Conference on Geosynthetics for Soil Improvements, New York, USA.

Lopes, M.L. and M. Ladeira, 1996(b) “Influence of the Confinement, Soil Density and Displacement Rate on Soil-Geogrid Interaction”, Geotextiles and Geomembranes, 14: 543-554.

Milligan, G.W.E. and E.P. Palmeira, 1987. “Prediction of Bond between Soil and Reinforcement”, Prediction and Performance in Geotechnical Engineering, Calgary.

Ochiai, H., J. Otani, S. Hayashic and T. Hirai, 1996. “The Pullout Resistance of Geogrids in Reinforced Soil”, Geotextiles and Geomembranes, pp: 19-42.

Raju, D.M. and R.J. Fannin, 1997. “Monotonic and Cyclic Pullout Resistance of Geogrids”, Geotechnique, 47: 331-337.

Sarsby, R.W., 1985. “The Influence of Aperture Size/Particle Size on the Efficiency of Grid Reinforcement”, 2nd Canadian Symposium on Geotextiles and Geomembrane.

TENAX Technical Reference GRID-TE-5 “Pullout Tests of Tenax Geogrids”, GeoSyntec Consultant, 1996.

Vesic, A.S., 1963. "Bearing Capacity of Deep Foundations in Sand", Highway Research Record No. 39, National Academy of Science, pp: 112-153.

Wilson-Fahmy, R., R.M. Koerner and L.J. Sansone, 1994. “Experimental Behavior of Polymeric Geogrids in Pullout”, Journal of Geotechnical Engineering, 120(4).